Journal of Fluorescence, Vol. 14, No. 1, January 2004 (©2004)

Fluorescence Measurements of Steady State Peroxynitrite Production Upon SIN-1 Decomposition: NADH Versus Dihydrodichlorofluorescein and Dihydrorhodamine 123

Francisco Javier Martin-Romero,[1] Yolanda Gutiérrez-Martin,[1] Fernando Henao,[1] and Carlos Gutiérrez-Merino[1,2]

Received August 31, 2003; revised September 27, 2003; accepted September 27, 2003

The production of peroxynitrite during 3-morpholinosydnonimine (SIN-1) decomposition can be continuously monitored, with a sensitivity ≤ 0.1 μM, from the kinetics of NADH fluorescence quenching in phosphate buffers, as well as in buffers commonly used with cell cultures, like Locke's buffer or Dulbecco's modified Eagle's medium (DMEM-F12). The half-time for peroxynitrite production during SIN-1 decomposition ranged from 14–18 min in DMEM-F12 (plus and minus phenol red) to 21.5 min in Locke's buffer and 26 min in DMEM-F12 supplemented with apotransferrin (0.1 mg/mL). The concentration of peroxynitrite reached a peak that was linearly dependent upon SIN-1 concentration, and that for 100 μM SIN-1 amounted to 1.4 ± 0.2 μM in Locke's buffer, 3.2–3.6 μM in DMEM-F12 (plus and minus phenol red) and 1.8 μM in DMEM-F12 supplemented with apotransferrin. Thus, the maximum concentration of peroxynitrite ranged from 1.2 to 3.6% of added SIN-1. NADH was found to be less sensitive than dihydrorhodamine 123 and 2′,7′-dichlorodihydrofluorescein diacetate to oxidation by H_2O_2, which is produced during SIN-1 decomposition in common buffers. It is shown that peroxynitrite concentration can be controlled (±5%) during predetermined times by using sequential SIN-1 pulses, to simulate chronic exposure of cells or subcellular components to peroxynitrite.

KEY WORDS: Peroxynitrite; 3-morpholinosydnonimine; NADH; fluorescence.

INTRODUCTION

Peroxynitrite ($ONOO^-$) has been shown to be involved in a number of pathologies in which cell death plays a major role [1–3]. However, $ONOO^-$ is a very short-lived chemical molecule in the buffered solutions used in cell culture studies (decomposition rate of 1.62 s^{-1} in phosphate buffer at pH 7 [3–6]), as well as in the cytosol (half-life lower than 0.1 s [3,6–8]). Thus, much of $ONOO^-$ added in a single pulse decomposes so rapidly that the efficiency of the $ONOO^-$ treatment is much lower than that expected to be attained under conditions where $ONOO^-$ release takes place smoothly, mimicking the "in vivo" situation. This has been demonstrated by studies carried out "in vitro" with isolated subcellular components [3,9,10], which have shown that for the same total exposure to $ONOO^-$, chronic treatment with micromolar $ONOO^-$ pulses produces much stronger effects than a single pulse of $ONOO^-$ even when this is added under strong vortexing conditions. An estimation of the exposure caused by a single addition of $ONOO^-$ can be done following the approach of Beckman *et al.* [9], which requires a previous measurement of the rate constant of the first-order process of $ONOO^-$ decay in the solution, a

[1] Departamento de Bioquímica y Biología Molecular y Genética, Facultad de Ciencias and Escuela de Ingenierías Agrarias, Universidad de Extremadura, Avenida de Elvas s/n, 06080-Badajoz, Spain.

[2] To whom correspondence should be addressed. E-mail: carlosgm@unex.es.

ABBREVIATIONS: DHR-123, dihydrorhodamine 123; DMEM-F12, Dulbecco's modified Eagle's medium; H_2DCF-DA, 2′,7′-dichlorodihydrofluorescein diacetate; SIN-1, 3-morpholinosydnonimine.

1053-0509/04/0100-0017/0

parameter that is dependent upon many variables, see, e.g. [3,5,7,11].

Exposure of cells to slowly released $ONOO^-$ can be mimicked by adding SIN-1, a peroxynitrite-producing agent, to the cell culture medium [12–15]. However, owing to the poor stability of SIN-1 in water solutions [16], and the time required to appropriately handle a number of cell culture dishes in many experimental designs, there is a need to measure the steady state $ONOO^-$ concentrations attained in the medium during treatments of cells with SIN-1. Noteworthy, the amplitude and duration of the $ONOO^-$ pulse produced by a given addition of SIN-1 is not well defined in previous studies, nor the maximum $ONOO^-$ concentration attained during SIN-1 decomposition, due to the lack of a simple method for directly measuring steady state $ONOO^-$ in the buffered solutions used for cell culture studies. An indirect approach following the kinetics of decomposition of SIN-1 has been developed [16], but the high reactivity of superoxide anion and nitric oxide with commonly used additives in bioassays recommend the use of a more direct approach.

Dihydrodichlorofluorescein (H_2DCF) and dihydrorhodamine 123 (DHR-123) can be used as indicators to measure peroxynitrite, as they are efficiently oxidized by $ONOO^-$ to their oxidized fluorescent forms dichlorofluorescein and rhodamine 123, respectively [17]. However, it has been noticed that both H_2DCF and DHR-123 can also be oxidized by many other reactive oxygen species (ROS) produced by cells subjected to oxidative stress [18–21].

In water solutions NADH is rapidly oxidized to the $NAD^\bullet$ radical by $ONOO^-$ or by $ONOO^-$-derived radicals, finally leading to the formation of NAD^+ [11]. We show that NADH can be used to follow the kinetics of $ONOO^-$ release upon SIN-1 decomposition, as well as to measure the time dependence of the steady state concentration of $ONOO^-$ attained during SIN-1 decomposition in standard media used in cell culture studies, with significant advantages over DHR-123 and H_2DCF. NADH measurements of peroxynitrite release during SIN-1 decomposition allows for the development of protocols with serial SIN-1 pulses to produce a controlled steady state $ONOO^-$ concentration for a pre-fixed time period.

MATERIALS AND METHODS

Preparation of Peroxynitrite

Peroxynitrite was synthesized as in [22]. Briefly, a solution of 0.6 M $NaNO_2$ was mixed at 4°C under vigorous stirring with an equal volume of 0.7 M H_2O_2 acidified with 0.6 M HCl. The product of this reaction was immediately stabilized by addition of an equal volume of 3 M NaOH. This solution was then treated with excess manganese dioxide (70–100 mg/mL) for 30 min at 4°C in order to eliminate the excess of H_2O_2. The concentration of H_2O_2 remaining after manganese dioxide treatment was measured spectrophotometrically, as described elsewhere [23] and found to be less than 0.1 moles H_2O_2 per mole of $ONOO^-$. Peroxynitrite solution was split into small aliquots and frozen at less than −25°C until use. Peroxynitrite concentration was measured spectrophotometrically in aliquots thawed immediately before using for the experiments reported in this paper, using an extinction coefficient of 1670 $M^{-1}\cdot cm^{-1}$ at 302 nm in 1.5 M NaOH [4]. $ONOO^-$ solutions were tested following the nitration of 4-hydroxyphenylacetic acid as described in [4].

Fluorescence and Absorbance Measurements

Fluorescence measurements have been carried out with a Perkin-Elmer 650-40 spectrofluorometer, equipped with a thermostated cell holder under continuous magnetic stirring. Absorbance measurements have been done with spectrophotometers (Kontron, Shimadzu) equipped with thermostated cell holders. NADH fluorescence has been measured with excitation and emission wavelengths of 340 and 460 nm, respectively. The composition of the buffers and media used for fluorescence and absorbance measurements were as follows:

Locke's K25 buffer composition: 134 mM NaCl /4 mM $NaHCO_3$ /25 mM KCl /10 mM HEPES /5 mM glucose /2.3 mM $CaCl_2$ /1 mM $MgCl_2$ (pH 7,4).

Dulbecco's modified Eagle's medium, DMEM/F12 (1:1), as supplied by Sigma Chemical Co. (St. Louis, MO.).

Materials

SIN-1 hydrochloride, NADH, dihydrorhodamine-123 (DHR-123), 4-hydroxyphenylacetic acid, DMEM-F12, apotransferrin, phenol red and hemin were supplied by Sigma Chemical Co. (St. Louis, MO). Superoxide dismutase and catalase were purchased from Roche Molecular Biochemicals (Mannheim, Germany). 2′,7′-dichlorodihydrofluorescein diacetate (H_2DCF-DA) was obtained from Molecular Probes (Groningen, Netherlands). All other chemicals used were of, at least, analytical grade and were supplied by Sigma or Merck.

RESULTS AND DISCUSSION

The ability to monitor $ONOO^-$ release by SIN-1 in a standard Locke K25 buffer is shown by the kinetics of

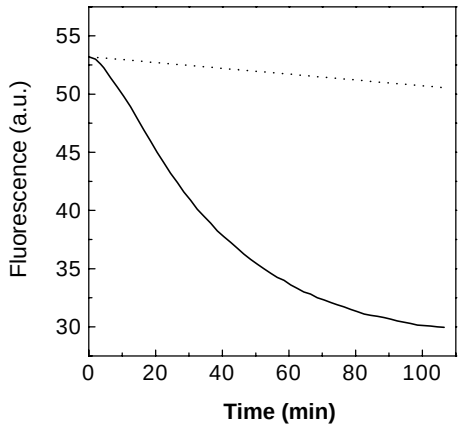

Fig. 1. *Kinetics of NADH oxidation by SIN-1.* Buffer: Locke K25 (pH 7.40, 37°C). Kinetics of NADH oxidation (followed by the quenching of NADH fluorescence) after addition of 15 μM SIN-1 to the buffered solution containing 25 μM NADH. The dotted line (reference line) corresponds to the air-dependent NADH oxidation upon irradiation at 340 nm in the same cuvette holder.

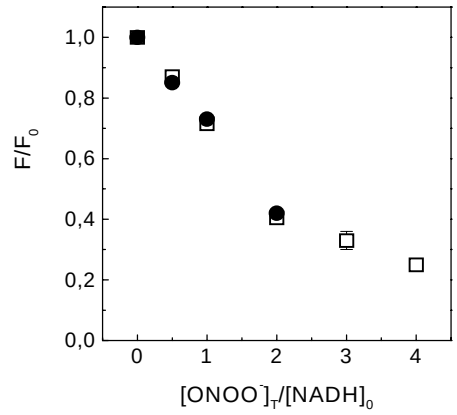

Fig. 2. *Stepwise titration of NADH fluorescence with ONOO$^-$* at low NADH concentrations. Buffer: 50 mM phosphate (pH 7) at 25°C. Quenching of the fluorescence of 1 μM (circles) and 5 μM (squares) NADH by addition of sequential 0.5 and 1 μM (circles) and 2.5 and 5 μM (squares) pulses of ONOO$^-$. In abscissa it has been plotted the ratio between added ONOO$^-$ concentration and the NADH concentration in the cuvette before the first ONOO$^-$ addition. The average errors of the data are indicated only in selected points, to avoid symbols confusion.

fluorescence quenching (Fig. 1) after SIN-1 addition to the solution containing NADH. The kinetics of NADH fluorescence quenching by SIN-1 overlapped with the kinetics of NADH oxidation to NAD^+ (monitored by the decay of absorbance at 340 nm, *data not shown*), and was more than 80% slowed down by addition of 1 U/μL superoxide dismutase plus 1.5 U/μl catalase (to ensure rapid superoxide anion removal) or by addition of 50 μM hemin (a NO scavenger). Therefore, NADH oxidation produced by SIN-1 is largely due to ONOO$^-$ formed upon SIN-1 decomposition, as noticed by Kirsch and de Groot [11].

This point was further confirmed by the rapid quenching of NADH fluorescence without significant distortion of the fluorescence emission spectra by addition of synthetic peroxynitrite (prepared as indicated in the Materials and Methods) under magnetic stirring, while addition of decomposed ONOO$^-$ (i.e., reverse order additions, with NADH added several minutes after dilution of ONOO$^-$ in the phosphate buffer) did not produce quenching of the NADH fluorescence. On average, with addition of synthetic ONOO$^-$ under magnetic stirring of the cuvette for fluorescence measurements we have obtained values of 0.25–0.32 for the ratio (oxidized NADH/total ONOO$^-$ added) at pH 7 (Fig. 2), in good agreement with the results obtained from absorbance measurements by Kirsch and de Groot [11]. The ratio between oxidized NADH and total ONOO$^-$ added is lower than one due to the kinetic competition between reaction of peroxynitrite with NADH and spontaneous peroxynitrite decomposition [11]. Because of the pH dependence of the rate of ONOO$^-$ decomposition [3], the sensitivity of NADH fluorescence to detect ONOO$^-$ increases about 2.4-fold at pH 7.5, e.g. it raises to 0.60–0.77 moles of oxidized NADH per mole of total ONOO$^-$ added under magnetic stirring (*data not shown*). Therefore, when peroxynitrite is produced homogeneously in the NADH-containing solution (such as during SIN-1 decomposition) the ratio of NADH oxidized/peroxynitrite should be even higher.

From the limiting values of absorbance and fluorescence after completion of the kinetic process of SIN-1 decomposition in Locke's buffer at pH 7.4 (Fig. 1) we can obtain that the efficiency of detection by NADH of the ONOO$^-$ produced upon SIN-1 decomposition is 80–90%, as one mole of ONOO$^-$ is produced per mole of SIN-1 [16,24,25]. This demonstrated that NADH is an excellent sensor for peroxynitrite in the submicromolar range.

The rate of production of ONOO$^-$ during SIN-1 decomposition in Locke's buffer at 37°C (Fig. 3(A)) has been calculated from the slope at different times (with a time window of 1 min) of the kinetics of quenching of NADH fluorescence (Fig. 1) and the efficiency of ONOO$^-$ detection by NADH indicated above. The maximum peak for ONOO$^-$ production is attained 20–30 min after SIN-1 addition to the solution, and it reaches 1.4 $\pm$ 0.2% of the added SIN-1 concentration (average of triplicate experiment). From Fig. 3A, the time course of total ONOO$^-$ production by SIN-1 can be obtained by integrating the area below the curve up to different times and the results are shown in Fig. 3B. The fact that the maximum rate of ONOO$^-$ production monitored with fluorescence quenching is linearly dependent upon SIN-1 concentration (Fig. 4), as expected on theoretical grounds since SIN-1

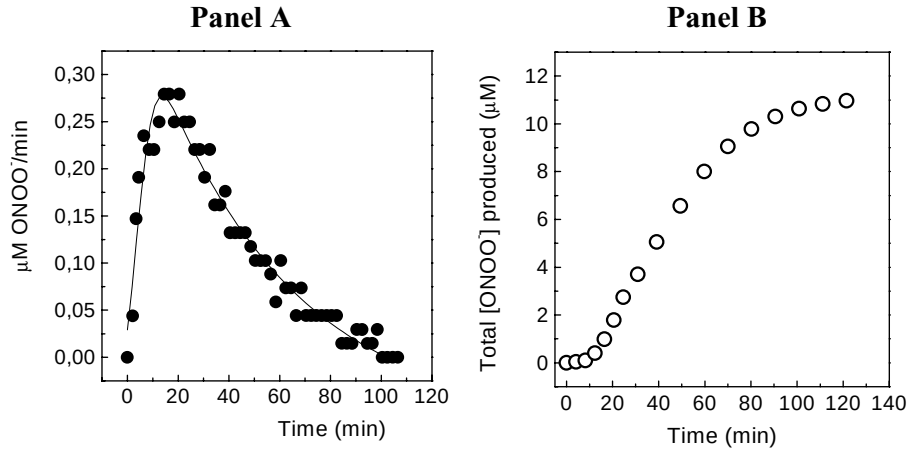

Fig. 3. *Peroxynitrite production during SIN-1 decomposition*. Panel A. Time dependence of $ONOO^-$ production, obtained from the decrease of NADH concentration (with 1 min intervals) derived from the kinetics of NADH fluorescence quenching shown in the Fig. 1, and the average fractional ratio [oxidized NADH]/$[ONOO^-]_T$ 0.90, derived from the data shown in the Fig. 1. The continuous line shows that the data can be fit to a modified gaussian (nonlinear least squares fit done with Origin^{TM} software, with a chi-square value of 0.00024). Panel B. Total $[ONOO^-]$ produced at different times after addition of SIN-1 to the solution, obtained from the plot shown in Panel A (areas up to the time indicated in the abscissa).

decomposition can be treated as a pseudo-first order kinetic process [16], further validates the reliability of these measurements. Identical results were obtained from measurements of the absorbance at 340 nm with higher SIN-1 and NADH concentrations (*data not shown*).

Phosphate-buffered saline or Locke's buffers are used with cell cultures only to do relatively fast functional measurements (like intracellular Ca^{2+} or reactive oxygen species measurements), but DMEM is widely used for most of mammalian cell culture handling and longer treatments. The efficiency of NADH for detection of peroxynitrite produced by SIN-1 decomposition in a standard supplemented DMEM, DMEM-F12 (1:1), as well as the maximum steady-state peroxynitrite concentration attained during SIN-1 decomposition and half-time of the SIN-1 decomposition process, have been obtained as indicated above and are listed in the Table I. Also included in this Table are the effects of DMEM-F12 supplementation with phenol red and apotransferrin, two commonly used additives to DMEM-F12 (see, e.g. [26,27]). These results showed that NADH can be readily used to monitor peroxynitrite generated from SIN-1 decomposition in DMEM, either using fluorescence quenching or absorbance measurements as indicated above.

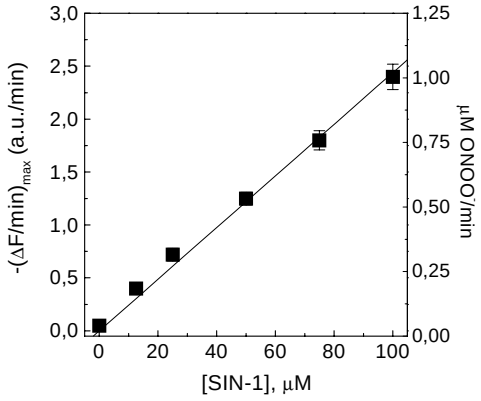

Fig. 4. Maximum steady state concentration of peroxynitrite attained during SIN-1 decomposition versus SIN-1 concentration. Results obtained from the kinetics of quenching of NADH fluorescence in Locke K25 (pH 7.40, 37°C), with an initial NADH concentration of 12.5–25 μM.

As H_2O_2 is produced simply by irradiation of cell culture media (such as DMEM-F12), particularly when supplemented with apotransferrin and other metalloproteins [28,29] and also during SIN-1 decomposition in commonly used buffers [11], it is particularly relevant to note that NADH is more resistant against oxidation by H_2O_2 in DMEM-F12 or Locke's buffer than the most frequently used fluorescent indicators for detection of peroxynitrite, namely DHR-123 and H_2DCF-DA. This is illustrated by the data shown in Fig. 5. The lack of significant oxidation of NADH by direct titration with H_2O_2 (up to 0.5 mM) in Locke's buffer or in DMEM-F12 (minus or plus apotransferrin) contrasts with the strong enhancement produced in the same range of H_2O_2 of the oxidation rate of DHR-123 or of H_2DCF-DA (Fig. 5). It is to be noted that both synthetic peroxynitrite and *in situ* generated peroxynitrite by SIN-1 decomposition oxidizes tertiary amines present

Table I. Production of Peroxynitrite During Decomposition of SIN-1 in Locke's Buffer and DMEM-F12 at pH 7.4 and 37°C

Medium	Efficiency[a]	Half-time[b] (min)	$[ONOO^-]_{max}$ (μM/min)[c]
Locke's buffer	0.85 ± 0.05	21.5 ± 0.5	1.4 ± 0.2
DMEM-F12	0.92 ± 0.05	17.5 ± 0.5	3.6 ± 0.2
DMEM-F12 plus phenol red	0.80 ± 0.05	14.5 ± 0.5	3.2 ± 0.2
DMEM-F12 plus 0.1 mg/mL apotransferrin	0.85 ± 0.05	26.0 ± 0.5	1.8 ± 0.2

Note. The data listed in this Table have been obtained from the kinetics of the decay of absorbance at 340 nm of 0.22 mM NADH upon addition of 100 μM SIN-1. Each data is the average of experiments done by triplicate.
[a] In moles NADH oxidized per mole of peroxynitrite released.
[b] Time for 50% of total peroxynitrite release.
[c] Obtained from the maximum slope per min of the kinetics of NADH oxidation.

in widely used cell culture media, with continuous H_2O_2 formation leading to near 200 μM after 2 h incubation with 1.5 mM SIN-1 [30]. Moreover, both DHR-123 and H_2DCF-DA showed significant oxidation when exposed to the excitation light-beam irradiation in the fluorescence cuvette in DMEM-F12 medium (Figs. 5B and C), at a rate equivalent to the rate of oxidation produced by 130 and 70 μM H_2O_2 for DHR-123 and H_2DCF-DA, respectively, thus, further complicating their use to reliably measure the submicromolar to micromolar steady state peroxynitrite concentrations attained during decomposition of up to 1 mM SIN-1 in commonly used cell culture medium (see above). It is worth-noting that SIN-1 concentrations of 0.5–1 mM are toxic for many cell cultures, see e.g. [12,15]. In addition, cell culture media are often supplemented with ascorbate and the DHR-123 radical is recycled by ascorbate, but not the $NAD^{\cdot}$ radical [31].

Therefore, we concluded that measurement of steady state $ONOO^-$ concentration using NADH fluorescence is more reliable than using H_2DCF-DA or DHR-123.

From the results shown above, it follows that to maintain a constant steady state concentration of $ONOO^-$ produced by SIN-1 during a predetermined time (for example, for cells culture exposure to $ONOO^-$ simulating a chronic $ONOO^-$ exposure) it is necessary to apply several SIN-1 pulses at defined time intervals. This is illustrated in

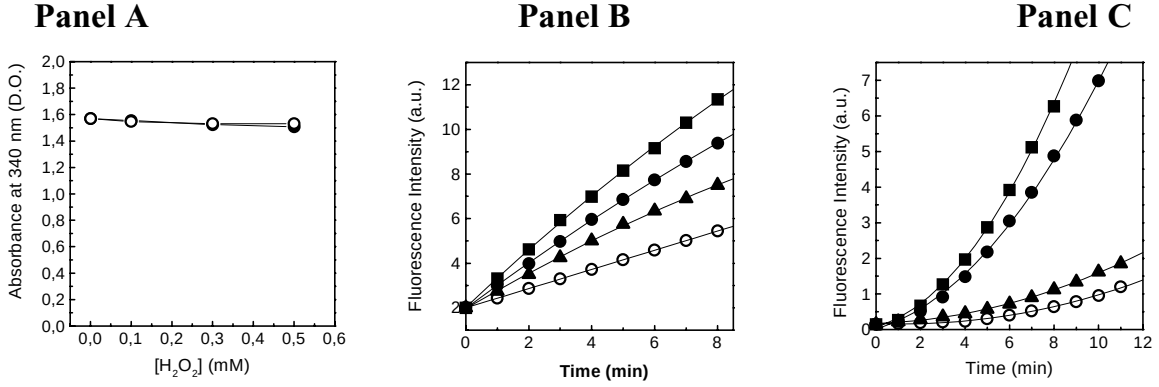

Fig. 5. Determination of the sensitivity to oxidation by H_2O_2 of NADH, DHR-123 and H_2 DCF-DA in DMEM-F12 at 37°C. Panel A. Titration with H_2O_2 of NADH. In the *Y*-axis is plotted the steady-state absorbance at 340 nm recorded for 5–10 min after addition of the H_2O_2 concentrations indicated in the abscissae to 0.22 mM NADH in DMEM-F12 (open circles) or in DMEM-F12 supplemented with 0.1 mg/mL apotransferrin (solid circles). Panel B. Kinetics of DHR-123 oxidation monitored by the increase of fluorescence (with excitation and emission wavelengths of 507 and 529 nm, respectively). The traces were obtained with 2.5 μM DHR-123 in DMEM-F12 in presence of the following H_2O_2 concentrations: none (open circles), 0.15 mM (solid up-triangles), 0.3 mM (solid circles), and 0.5 mM (solid squares). Panel C. Kinetics of H_2DCF-DA oxidation monitored by the increase of fluorescence (with excitation and emission wavelengths of 504 and 529 nm, respectively). The traces were obtained with 2 μM H_2DCF-DA in DMEM-F12 in presence of the following H_2O_2 concentrations: none (open circles), 0.1 mM (solid up-triangles), 0.3 mM (solid circles), and 0.5 mM (solid squares).

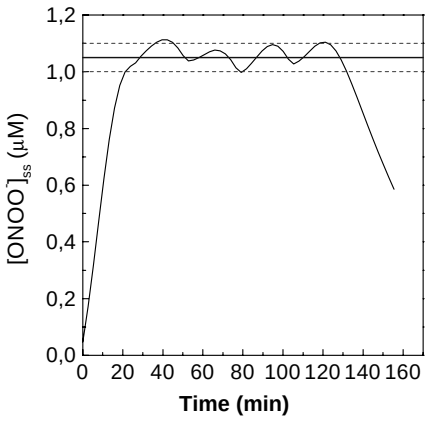

Fig. 6. Sequential serial SIN-1 pulses protocol to maintain a nearly constant steady state $ONOO^-$ concentration, $[ONOO^-]_{ss}$, of 1.05 ± 0.05 μM during approximately 105 min. Plot derived from the sum of the five modified gaussian peaks corresponding to the kinetics of production of $ONOO^-$ (Fig. 3A) by five sequential pulses of 60, 20, 20, 25, and 25 μM SIN-1 applied at times 0, 26.4, 52.7, 79.1, and 105.4 min, respectively.

the Fig. 6 with a simulation of the time dependence of $ONOO^-$ production giving a steady state concentration of $ONOO^-$ of 1.05 ± 0.05 μM during a time window of approximately 1 hr. Modifying each of the SIN-1 pulses by the same factor, n, while leaving the times of each pulse application unchanged, will result in a steady state concentration of $ONOO^-$ of $n \cdot (1.05 \pm 0.05)$ μM during the same time window. For example, to obtain a steady state concentration of $ONOO^-$ of 2.1 ± 0.1 μM during the time window indicated in the Fig. 6, the size of each SIN-1 pulse should be multiplied by two and applied at the times indicated in the legend to this Figure.

CONCLUSIONS

The results presented in this paper show that NADH can be used as a tool to monitor peroxynitrite in buffered solutions currently used for cells and subcellular organelles activity assays, with a limiting sensitivity lower than 0.1 μM peroxynitrite at pH 7.4 when SIN-1 is used to generate $ONOO^-$ homogeneously in the solution. NADH is by far less sensitive than DHR-123 or H_2DCF-DA to interferences coming from the concomitant production of H_2O_2 during SIN-1 decomposition. In addition, as SIN-1 solutions are highly unstable at neutral pH, this provides a useful and rapid test for the actual concentration of SIN-1 stock solutions before carrying out experiments with cell cultures or doing bioassays.

Finally, during the kinetic process of SIN-1 decomposition the peak $ONOO^-$ concentrations produced by SIN-1 in Locke's buffer have been found to be only 1.4 $\pm$0.2% of the total SIN-1 concentration added to the solution, and from the time dependence of the $ONOO^-$ concentration attained in the solution, serial SIN-1 pulse protocols can be developed to maintain the $ONOO^-$ steady state concentration within a narrow range (e.g. $\pm$5%) during different times, in order to simulate chronic long term exposure of cells or subcellular components to $ONOO^-$.

ACKNOWLEDGMENTS

This work has been supported by Grants BMC2000-0547 of the Spanish Ministerio de Ciencia y Tecnologia, and IPR00A091 of the Junta de Extremadura. Y.G.-M. is recipient of a Predoctoral Fellowship of the Spanish Ministerio de Educación y Cultura.

REFERENCES

1. J. S. Beckman, M. Carson, C. D. Smith, and W. H. Koppenol (1993). ALS, SOD and peroxynitrite. *Nature* **364**(6438), 584.
2. B. Halliwell (1997). What nitrates tyrosine? Is nitrotyrosine specific as a biomarker of peroxynitrite formation in vivo? *FEBS Lett.* **411**(2/3), 157–160.
3. M. P. Murphy, M. A. Packer, J. L. Scarlett, and S. W. Martin (1998). Peroxynitrite: A biologically significant oxidant. *Gen. Pharmacol.* **31**(2), 179–186.
4. R. M. Uppu and W. A. Pryor (1996). Synthesis of peroxynitrite in a two-phase system using isoamyl nitrite and hydrogen peroxide. *Anal. Biochem.* **236**(2), 242–249.
5. S. Pfeiffer, A. C. Gorren, K. Schmidt, E. R. Werner, B. Hansert, D. S. Bohle, and B. Mayer (1997). Metabolic fate of peroxynitrite in aqueous solution. Reaction with nitric oxide and pH-dependent decomposition to nitrite and oxygen in a 2:1 stoichiometry. *J. Biol. Chem.* **272**(6), 3465–3470.
6. W. H. Koppenol, J. J. Moreno, W. A. Pryor, H. Ischiropoulos, and J. S. Beckman (1992). Peroxynitrite, a cloaked oxidant formed by nitric oxide and superoxide. *Chem. Res. Toxicol.* **5**(6), 834–842.
7. G. E. Arteel, K. Briviba, and H. Sies (1999). Protection against peroxynitrite *FEBS Lett.* **445**(2/3), 226–230.
8. R. Radi (1998). Peroxynitrite reactions and diffusion in biology. *Chem. Res. Toxicol.* **11**(7), 720–721.
9. J. S. Beckman, J. Chen, H. Ischiropoulos, and J. P. Crow (1994). Oxidative chemistry of peroxynitrite. *Methods Enzymol.* **233,** 229–240.
10. Y. Gutierrez-Martin, F. J. Martin-Romero, F. Henao, and C. Gutierrez-Merino (2002). Synaptosomal plasma membrane Ca^{2+} pump activity inhibition by repetitive micromolar $ONOO^-$ pulses. *Free Radical. Biol. Med.* **32**(1), 46–55.
11. M. Kirsch and H. de Groot (1999). Reaction of peroxynitrite with reduced nicotinamide nucleotides, the formation of hydrogen peroxide. *J. Biol. Chem.* **274**(35), 24664–24670.
12. S. A. Lipton, Y. B. Choi, Z. H. Pan, S. Z. Lei, H. S. Chen, N. J. Sucher, J. Loscalzo, D. J. Singel, and J. S. Stamler (1993). A redox-based mechanism for the neuroprotective and neurodestructive effects of nitric oxide and related nitroso-compounds. *Nature* **364**(6438), 626–632.
13. L. Brunelli, J. P. Crow, and J. S. Beckman (1995). The comparative toxicity of nitric oxide and peroxynitrite to Escherichia coli. *Arch. Biochem. Biophys.* **316**(1), 327–334.
14. A. J. Gow, Q. Chen, M. Gole, M. Themistocleous, V. M. Lee, and H. Ischiropoulos (2000). Two distinct mechanisms of nitric

oxide-mediated neuronal cell death show thiol dependency. *Am. J. Physiol. Cell. Physiol.* **278**(6), C1099–C1107.
15. J. L. Trackey, T. F. Uliasz, and S. J. Hewett (2001). SIN-1-induced cytotoxicity in mixed cortical cell culture: Peroxynitrite-dependent and-independent induction of excitotoxic cell death. *J. Neurochem.* **79**(2), 445–455.
16. A. Schrammel, S. Pfeiffer, K. Schmidt, D. Koesling, and B. Mayer (1998). Activation of soluble guanylyl cyclase by the nitrovasodilator 3-morpholinosydnonimine involves formation of S-nitrosoglutathione. *Mol. Pharmacol.* **54**(1), 207–212.
17. J. P. Crow (1997). Dichlorodihydrofluorescein and dihydrorhodamine 123 are sensitive indicators of peroxynitrite in vitro: Implications for intracellular measurement of reactive nitrogen and oxygen species. *Nitric Oxide* **1**(2), 145–157.
18. J. A. Royall and H. Ischiropoulos (1993). Evaluation of 2′,7′-dichlorofluorescin and dihydrorhodamine 123 as fluorescent probes for intracellular H_2O_2 in cultured endothelial cells. *Arch. Biochem. Biophys.* **302**(2), 348–355.
19. D. Jourd'heuil, L. Mills, A. M. Miles, and M. B. Grisham (1998). Effect of nitric oxide on hemoprotein-catalyzed oxidative reactions. *Nitric Oxide* **2**(1), 37–44.
20. S. L. Hempel, G. R. Buettner, Y. Q. O'Malley, D. A. Wessels, and D. M. Flaherty (1999). Dihydrofluorescein diacetate is superior for detecting intracellular oxidants: comparison with 2′,7′-dichlorodihydrofluorescein diacetate, 5(and 6)-carboxy-2′,7′-dichlorodihydrofluorescein diacetate, and dihydrorhodamine 123. *Free Radical. Biol. Med.* **27**(1/2), 146–159.
21. T. Ohashi, A. Mizutani, A. Murakami, S. Kojo, T. Ishii, and S. Taketani (2002). Rapid oxidation of dichlorodihydrofluorescin with heme and hemoproteins: Formation of the fluorescein is independent of the generation of reactive oxygen species. *FEBS Lett.* **511**(1–3), 21–27.
22. R. Radi, J. S. Beckman, K. M. Bush, and B. A. Freeman (1991). Peroxynitrite oxidation of sulfhydryls. The cytotoxic potential of superoxide and nitric oxide. *J. Biol. Chem.* **266**(7), 4244–4250.
23. A. Claiborne (1985). In R. A. Greenwald (Ed.), *Handbook of Methods for Oxygen Radical Research*, CRC Press, Boca Raton, FL, pp. 283–284.
24. H. Bohn and K. Schonafinger (1989). Oxygen and oxidation promote the release of nitric oxide from sydnonimines. *J. Cardiovasc. Pharmacol.* **14** Suppl. 11, S6–S12.
25. M. Feelisch, J. Ostrowski, and E. Noack (1989). On the mechanism of NO release from sydnonimines. *J. Cardiovasc. Pharmacol.* **14**(Suppl 11), S13–S22.
26. F. J. Martin-Romero, E. Garcia-Martin, and C. Gutierrez-Merino (2002). Inhibition of oxidative stress produced by plasma membrane NADH oxidase delays low-potassium-induced apoptosis of cerebellar granule cells. *J. Neurochem.* **82**(3), 705–715.
27. F. J. Martin-Romero, B. Santiago-Josefat, J. Correa-Bordes, C. Gutierrez-Merino, and P. Fernandez-Salguero (2000). Potassium-induced apoptosis in rat cerebellar granule cells involves cell-cycle blockade at the G1/S transition. *J. Mol. Neurosci.* **15**(3), 155–165.
28. B. Halliwell (2003). Oxidation stress in cell culture: An underappreciated problem? *FEBS Lett.* **540**(1–3), 3–6.
29. L. Hua Long and B. Halliwell (2001). Oxidation and generation of hydrogen peroxide by thiol compounds in commonly used cell culture media. *Biochem. Biophys. Res. Commun.* **286**(5), 991–994.
30. M. Kirsch, E. E. Lomonosova, H. G. Korth, R. Sustmann, and H. de Groot (1998). Hydrogen peroxide formation by reaction of peroxynitrite with Hepes and related tertiary amines. *J. Biol. Chem.* **273**(21), 12716–12724.
31. M. Kirsch and H. de Groot (2000). Ascorbate is a potent antioxidant against peroxynitrite-induced oxidation reactions. Evidence that ascorbate acts by re-reducing substrate radicals produced by peroxynitrite. *J. Biol. Chem.* **275**(22), 16702–16708.